Virchows Archiv A Pathol Anat (1993) 422:73–80

Virchows Archiv A
Pathological Anatomy and Histopathology

Immunocytochemical study of membrane skeletons in abnormally shaped erythrocytes as revealed by a quick-freezing and deep-etching method

Shinichi Ohno, Nobuo Terada, Yasuhisa Fujii, Hideho Ueda, Hirofumi Kuramoto, and Nanako Kamisawa

Department of Anatomy, Yamanashi Medical University, 1110 Shimokato, Tamaho, Yamanashi 409-38, Japan

Received September 17, 1992 / Accepted October 8, 1992

Summary. Ultrastructures of membrane skeletons in spherocytic and elliptocytic erythrocytes were investigated immunocytochemically. Erythrocytes obtained from patients with hereditary spherocytosis (HS) and hereditary elliptocytosis (HE) were split open mechanically to obtain exposed cytoplasmic sides of erythrocyte membranes and were immunostained with anti-spectrin antibody. Replica membranes were prepared by a quick-freezing and deep-etching method and were checked by electron microscopy. The in situ membrane skeletons of normal erythrocytes consisted mainly of reticular patterns of spectrin filaments, which formed networks on the cytoplasmic sides of the cell membrane. In contrast, the membrane skeletons of abnormally shaped erythrocytes (HS and HE) were much less filamentous and more granular than those of normal erythrocytes. This abnormal organization in erythrocyte membrane skeletons may be one of the factors that induce abnormally shaped erythrocytes in HS and HE patients.

Key words: Elliptocyte – Spherocyte – Membrane skeleton – Quick-freezing

Introduction

Morphological studies have demonstrated that the membrane skeleton of normal erythrocytes has a finely reticular structure (Byers and Branton 1985; Fujikawa 1983; Liu et al. 1987; Lupu and Constantinescu 1989; Nermut 1981; Shen et al. 1984, 1986; Tsukita et al. 1980; Ursitti et al. 1991). The network consists mainly of proteins such as spectrin, actin, band 4.1, band 4.9, ankyrin and tropomyosin (Bennett 1985, 1989; Delaunay et al. 1990; Goodman and Shiffer 1983; Marchesi 1983; McGuire and Agre 1988). The spectrin molecules are usually in the form of tetramers, each composed of two filamentous molecules (dimers) and joined in head-to-head fashion. The spectrin tetramers are also bound to actin, band 4.1 and band 4.9 to form two-dimensional networks, which are attached to band 3 in the lipid bilayer by the action of a cross-linking protein, ankyrin. It is thought that mutual binding of these proteins serves the purpose of regulating the structure of the membrane skeleton and thus maintains the shape of erythrocytes (Bennett 1985, 1989; Delaunay et al. 1990; Fowler 1986; Goodman and Shiffer 1983; Marchesi 1983). Biochemical studies have demonstrated that a variety of different genetic defects of erythrocyte proteins are responsible for abnormalities in shape of erythrocytes such as hereditary spherocytosis (HS) and hereditary elliptocytosis (HE) (Delaunay et al. 1990; Goodman and Shiffer 1983; Iolascon et al. 1992; McGuire and Agre 1988). Actually, decreased quantity of spectrin (Agre et al. 1985, 1986), deficiency of spectrin tetramer formation (Liu et al. 1982) and abnormalities in spectrin-actin-band 4.1 binding (Goodman et al. 1982; McGuire et al. 1988; Tchernia et al. 1981) have been reported to be related to these pathological conditions. The ultrastructure of spectrin networks in abnormally shaped erythrocytes has been described (Liu et al. 1990).

A new erythrocyte-splitting technique for the ultrastructural study of erythrocyte membranes has been developed recently (Ohno 1992), in which the erythrocytes are split open mechanically. After removing intracytoplasmic soluble proteins, the replica membranes of cytoplasmic sides are prepared by a quick-freezing and deep-etching method (Lupu and Constantinescu 1989; Nermut 1981; Ohno 1992; Ursitti et al. 1991). This permits a three-dimensional observation of the ultrastructure of erythrocyte membranes at high resolution, as previously reported in other cultured cells (Ohno 1985; Ohno and Fujii 1990, 1991; Ohno and Takasu 1989). In the present study, using the erythrocyte-splitting technique and the quick-freezing and deep-etching method, we performed an immunocytochemical study of the cytoplasmic aspect of abnormally shaped erythrocyte membranes obtained from patients with HS or HE.

Correspondence to: S. Ohno

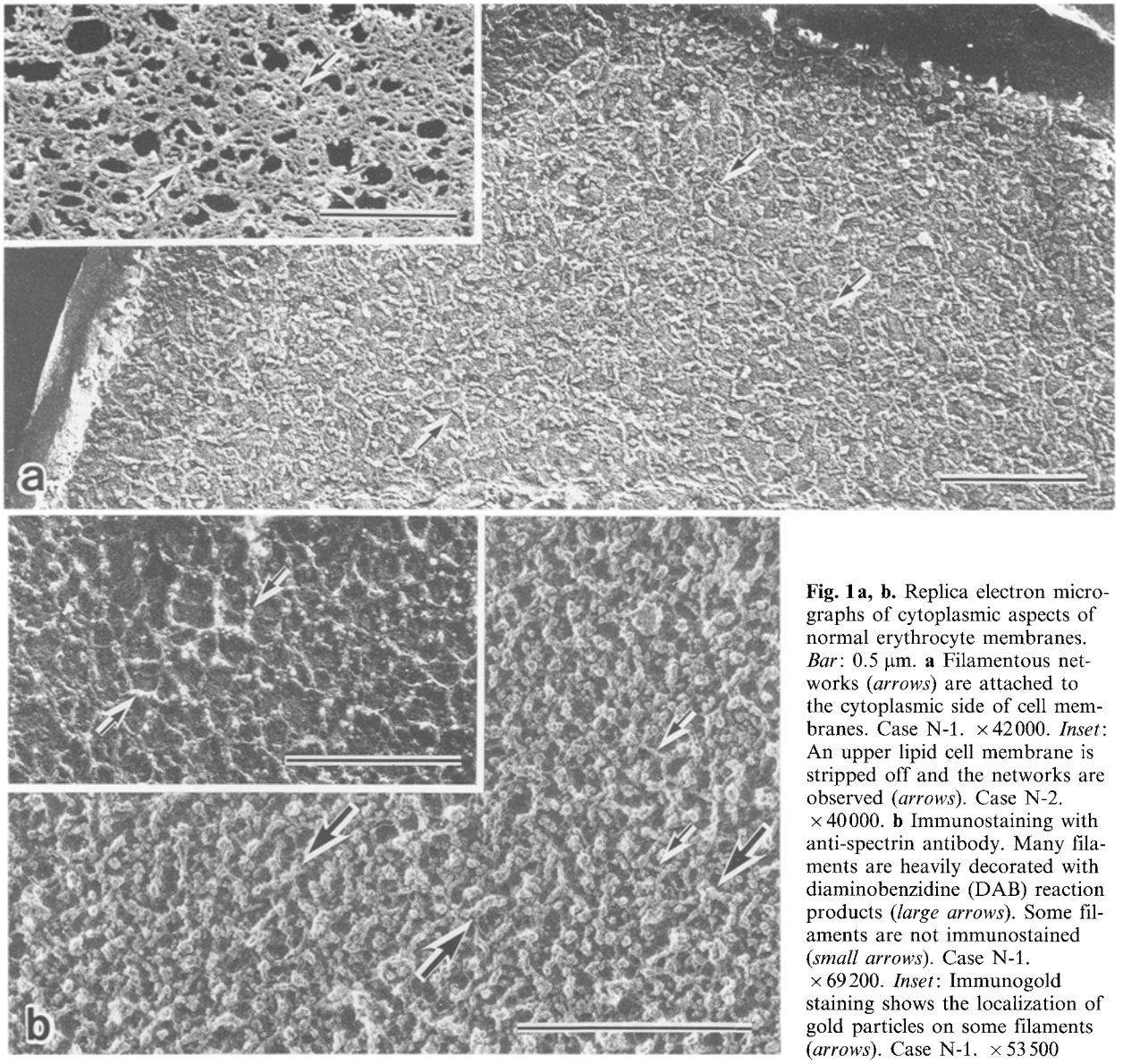

Fig. 1a, b. Replica electron micrographs of cytoplasmic aspects of normal erythrocyte membranes. *Bar*: 0.5 μm. **a** Filamentous networks (*arrows*) are attached to the cytoplasmic side of cell membranes. Case N-1. ×42000. *Inset*: An upper lipid cell membrane is stripped off and the networks are observed (*arrows*). Case N-2. ×40000. **b** Immunostaining with anti-spectrin antibody. Many filaments are heavily decorated with diaminobenzidine (DAB) reaction products (*large arrows*). Some filaments are not immunostained (*small arrows*). Case N-1. ×69200. *Inset*: Immunogold staining shows the localization of gold particles on some filaments (*arrows*). Case N-1. ×53500

Materials and methods

Included in this study were three patients with HS (one male, two females, 35–78 years of age), two patients with HE (one male and one female, 42 and 74 years of age) from several families and two healthy volunteers (one male and one female, 28 and 42 years of age). Some of the laboratory data in these seven cases are shown in Table 1. The HS patients exhibited decreased haemoglobin concentration and increased reticulocyte counts, indicative of haemolytic anaemia. In all cases, spherocytes accounted for over 60% of the erythrocytes seen in peripheral blood smears. None of the HS patients had undergone splenectomy. The HE patients had anaemia, with over 80% elliptocytes in peripheral blood smears. Neither of these patients had been splenectomized. The two healthy adults had no anaemia and had normal discoid erythrocytes in peripheral blood smears, as previously reported (Ohno 1992).

From each case, 10 ml venous blood was withdrawn with a syringe containing 0.1% heparin. The blood was washed and centrifuged (3000 *g*, 10 min) three times with the phosphate buffer with magnesium/EGTA (150 mM sodium chloride/5 mM sodium dihydrogen phosphate/2 mM sodium azide/2 mM magnesium chloride/1 mM EGTA, pH 7.5) to obtain erythrocyte pellets. They were fixed with 2% paraformaldehyde in 0.1 M phosphate buffer, pH 7.4, (PB) for 10 min and washed three times by centrifugation to prepare erythrocyte pellets.

In order to prepare replicas, erythrocytes were split open by using a new method devised by one of the present authors (Ohno

Table 1. Laboratory data of normal controls (N) and hereditary spherocytosis (HS) and hereditary elliptocytosis (HE) patients

Case	Sex	Age (years)	Hb (g/dl)	Ret (‰)	T-B/I-B (mg/dl)	Abnormal shape (%)
N-1	M	42	15.7	2	0.2/0.1	0
N-2	F	28	12.1	10	0.5/0.2	0
HS-1	F	35	9.2	110	2.8/2.3	60–70
HS-2	F	40	13.0	106	2.5/1.7	60–70
HS-3	M	78	11.8	55	2.1/1.3	70–80
HE-1	M	42	9.8	28	0.4/0.3	80–90
HE-2	F	74	10.4	78	2.2/1.5	80–90

Hb, Haemoglobin; Ret (‰), reticulocytes per 1000 cells; T-B, total bilirubin; I-B, indirect bilirubin

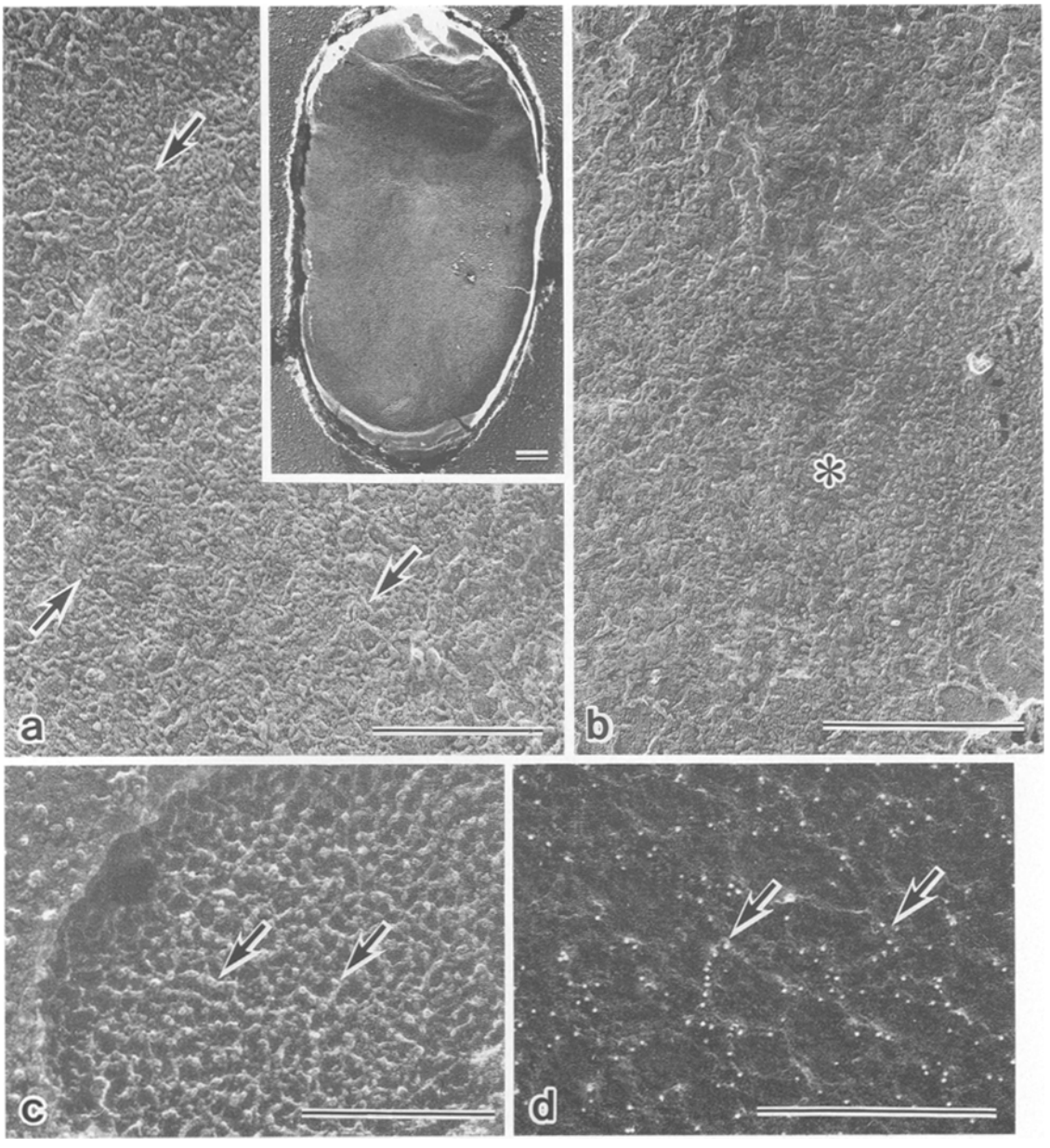

Fig. 2a–d. Replica electron micrographs of elliptocytic erythrocytes. *Bar*: 0.5 μm. **a** Membrane skeletons (*arrows*) are less filamentous than those of normal erythrocytes. Case HE-1. ×47900. *Inset*: Surface view of an elliptocytic erythrocyte. Case HE-1. ×7500. **b** In another case, HE-2, membrane skeletons are more granular in some areas (*asterisk*). ×56700. **c** Immunostaining of spectrin with peroxidase labelling. Filamentous structures are decorated with DAB reaction products (*arrows*). Case HE-1. ×54000. **d** Immunostaining of spectrin with colloidal gold labelling. Gold particles are mainly localized on filamentous networks (*arrows*). Case HE-1. ×67500

1985, 1992; Ohno and Fujii 1990). Briefly, a coverslip was coated with 3-aminopropyl triethoxysilane and 1% glutaraldehyde so that erythrocyte membranes could readily adhere to the glass surface. A drop of the erythrocyte pellet was put on the coverslip, and another coverslip was superimposed on it to sandwich the erythrocytes. The overlying coverslip was gently pressed with a pincette to make the erythrocytes adhere to both coverslips and the PB was allowed to run between them. The coverslips were then detached and the erythrocytes were split open. After being deprived of soluble proteins by thorough washing with phosphate buffered saline (PBS), the erythrocytes were fixed with 2.5% glutaraldehyde in PB for 30 min and stored in PBS at 4° C.

Immunoperoxidase labelling was carried out on the erythrocyte membranes on coverslips. They were washed with PBS and treated with 0.1 M lysine in PB for 30 min to block the free aldehyde residues of glutaraldehyde. They were then immunostained firstly with anti-spectrin polyclonal antibody from rabbits (Transformation Res., Mass., USA) and secondarily with goat anti-rabbit IgG coupled to peroxidase (E-Y Laboratories, Calif., USA). They were again fixed with 2.5% glutaraldehyde and were incubated in the diaminobenzidine and hydrogen peroxide solution for 1 min (Ohno and Takasu 1989). As the immunostaining controls, normal rabbit serum and PBS were used in the same way without the primary antibody (data not shown).

Immunogold labelling was carried out with the anti-spectrin antibody and goat anti-rabbit IgG coupled to 8 nm colloidal gold particles (E-Y Laboratories) for 5 h at room temperature. They were washed extensively in PBS for 1 h to remove unbound gold

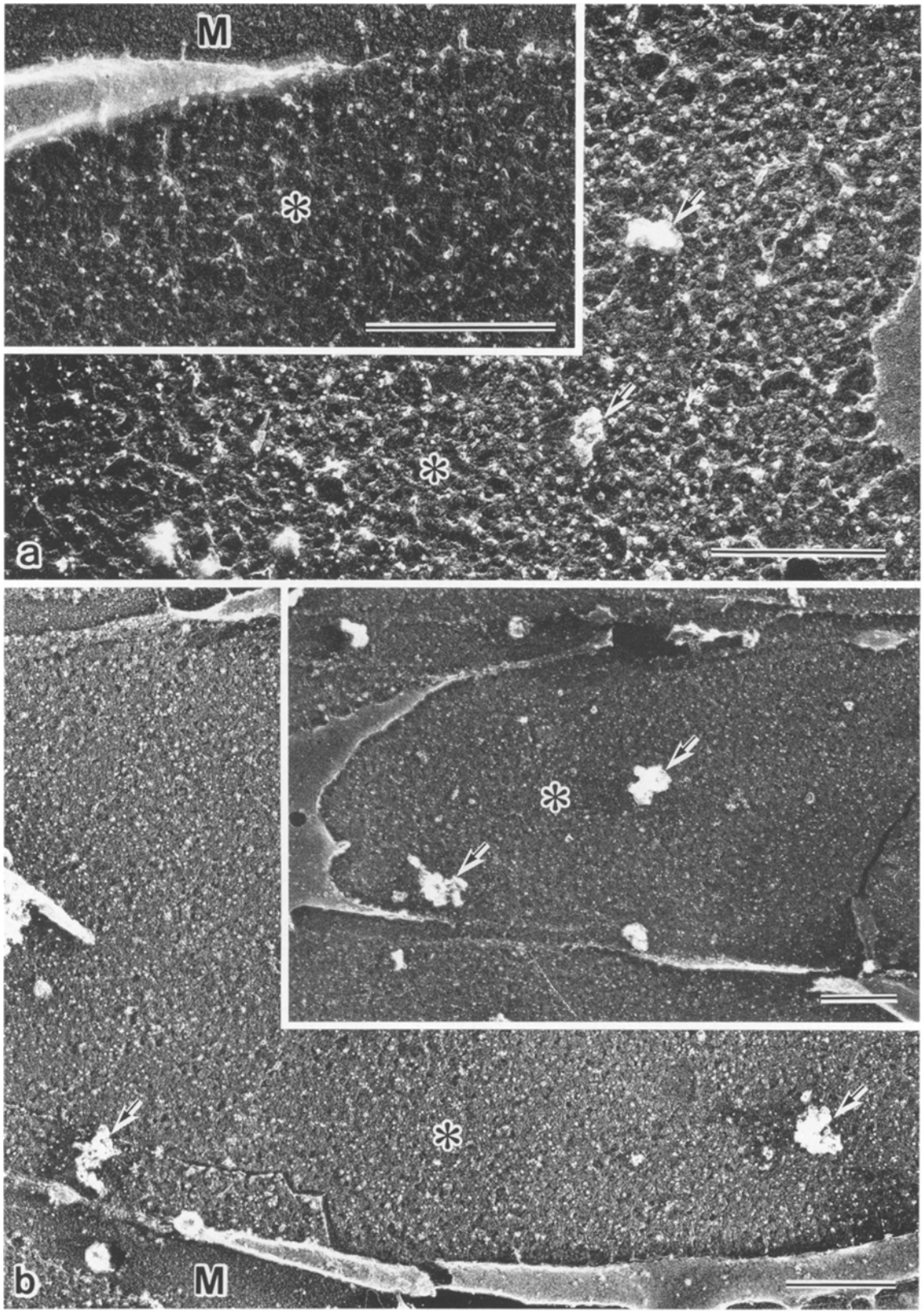

Fig. 3a, b. Replica electron micrographs of different elliptocytic membranes, which are immunostained with anti-spectrin antibody and secondary gold-conjugated antibody. *Bar*: 0.5 μm. **a** Many gold particles are located on disorganized networks attached to the cytoplasmic side (*asterisk*). Membrane debris is often observed (*arrows*). Case HE-1. ×56600. *Inset*: Case HE-2. ×61600. *M*, Extracellular matrix. **b** Gold particles are randomly located on non-filamentous cytoplasmic sides (*asterisk*) of typical elliptocytic membranes. *Arrows*, Membrane debris; *M*, extracellular matrix. Case HE-1. ×35500. *Inset*: Case HE-2. ×24900

particles and fixed with 2.5% glutaraldehyde in PB for 15 min to stabilize the binding of antigen-antibody-gold complex.

For quick-freezing and deep-etching the prepared erythrocytes were immersed in distilled water for removal of salts and further in 10% methanol to prevent the formation of ice crystals (Ohno 1992) before being quickly frozen. The coverslip with the split erythrocytes was mounted on copper holders and rapidly immersed in a liquid isopentane-propane mixture (−193° C) cooled in liquid nitrogen after removal of excess fluid with filter paper. These quickly frozen specimens were then transferred to a stage precooled at −170° C in an Eiko FD-3S machine and deeply-etched under the vacuum conditions of $2\text{-}6X10^{-7}$ Torr at −95° C for 30–60 min. A replica of the exposed cytoplasmic side was then prepared by evaporation of platinum at an angle of 25° and subsequently of carbon at an angle of 90°.

The replica membranes, upon being taken out of the apparatus, were immediately coated with 2% collodion diluted with amylacetate and dried. They were immersed in a solution of commercialized household bleach to digest away cell membrane components. The collodion-filmed replicas were washed twice with distilled water, placed on copper grids coated with Formvar and finally treated with amylacetate to dissolve out the collodion. The replica membranes were examined in Hitachi HS-9 and H-700 electron microscopes at accelerating voltages of 75–100 kV. Electron micrographs of erythrocyte membranes were printed from reversed negatives so that areas of platinum deposition look bright, in contrast with dark backgrounds.

The morphometric analysis to count the intersection of more than three spectrin filaments was carried out with a Digigramer-G analyser (Mutoh, Tokyo, Japan), as reported before (Ohno 1992). Moreover, the number of immunogold particles was counted in the same system. All values were expressed as means ± standard deviation.

Results

Figure 1 illustrates cytoplasmic aspects of normal erythrocyte membranes. Filamentous structures arranged in reticular patterns were attached to the lipid cell membrane (Fig. 1 a). These filaments varied in thickness and length. They were immunostained with anti-spectrin antibody followed by the immunoperoxidase method (Fig. 1 b) and the immunogold method (Fig. 1 b, inset). Figures 2 and 3 illustrate cytoplasmic aspects of elliptocytic erythrocytes. Their ultrastructures, when compared with those of normal erythrocyte membranes, were different with a less filamentous and more granular appearance of the membrane skeleton (Fig. 2a, b). In some parts, filamentous structures were stretched out to form reticular patterns, which were immunostained with anti-spectrin antibody followed by the immunoperoxidase (Fig. 2c) and the immunogold methods (Fig. 2d). In other parts, their arrangement was less orderly than that seen in normal erythrocytes (Fig. 3a). Immunogold par-

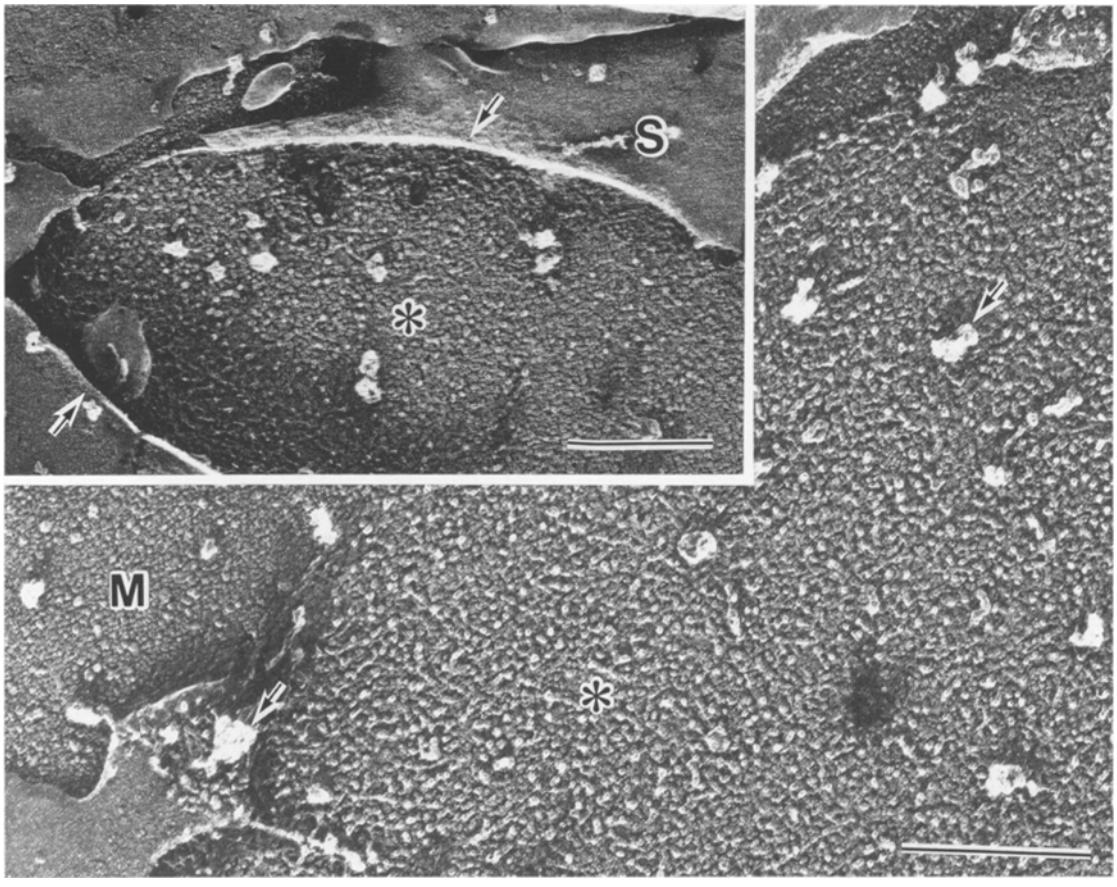

Fig. 4. Replica electron micrographs of spherocytic erythrocytes. *Bar:* 0.5 μm. Cytoplasmic aspects of erythrocyte membranes (*asterisks*) are less filamentous and more granular than those of control erythrocytes, as shown in Fig. 1. Membrane debris is often observed (*arrows*). *M*, Extracellular matrix. Case HS-1. ×49400. *Inset*: In another case, HS-2, an upper erythrocyte membrane is partially removed (*arrows*). Granular, but not filamentous, structures are obviously observed (*asterisk*). *S*, Erythrocyte membrane surface. ×39200

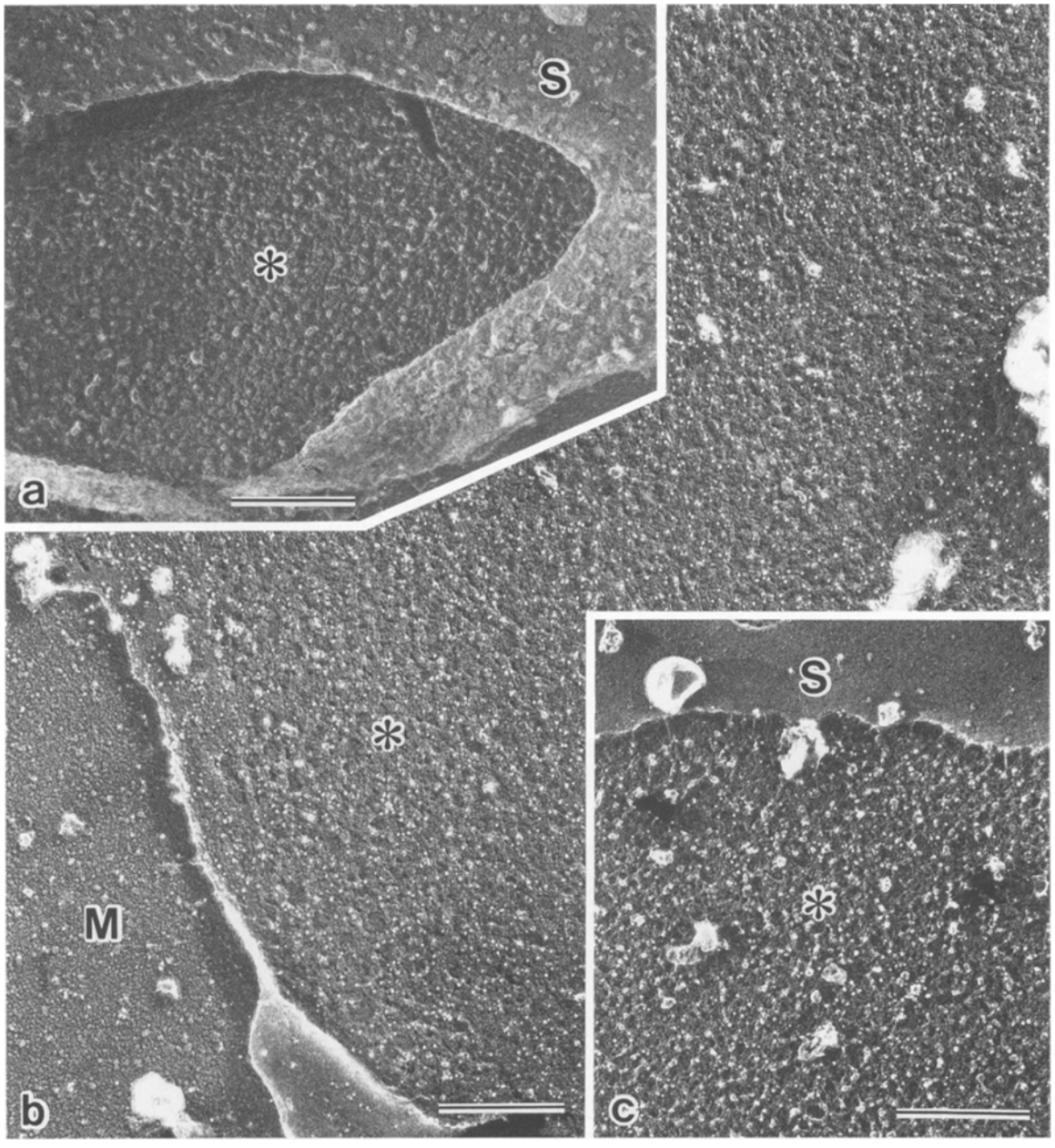

Fig. 5a–c. Replica electron micrographs of spherocytic erythrocyte membranes, which are immunostained with anti-spectrin antibody. *Bar*: 0.5 μm. **a** Immunostaining of spectrin with peroxidase labelling. Filamentous structures are not identified on the cytoplasmic side of erythrocyte membranes (*asterisk*). *S*, Erythrocyte membrane surface. Case HS-1. ×37500. **b** Immunostaining of spectrin with colloidal gold labelling. Many immunogold particles are randomly located on the cytoplasmic side of membranes (*asterisk*). Some non-specific gold particles are also located on the outside of erythrocytes (*M*). Case HS-1. ×36900. **c** Immunogold labelling. No filamentous structures are observed (*asterisk*). *S*, Erythrocyte membrane surface. Case HS-3. ×37400

ticles were randomly attached to the cytoplasmic side of typical elliptocytic erythrocyte membranes (Fig. 3b).

Figures 4 and 5 illustrate cytoplasmic aspects of spherocytic erythrocytes. While filamentous structures were less organized into reticular patterns (Fig. 4), some were granular, when compared with those seen in Fig. 1a. In a spherocyte, the erythrocyte membrane was partially removed and the ultrastructure of the cytoplasmic sides was observed through the membrane crevice (Fig. 4, inset). The cytoplasmic aspects were predominantly more granular in appearance than those of normal erythrocytes. They were immunostained with anti-spectrin antibody followed by the immunoperoxidase method (Fig. 5a) and the immunogold method (Fig. 5b, c).

Table 2 summarizes morphometric data on the numbers of filament intersections and gold particles. The number of the intersections is significantly different between normal controls and HS or HE patients (Table 2a, $P<0.001$). However, the number of immunogold particles is not significantly different among them, though their means of the patients are slightly decreased (Tab-

Table 2. Morphometric data of control erythrocytes and abnormal erythrocytes with HS or HE

	Number of intersections[a] (mean ± SD, $n=75$)	Number of gold particles[b] (mean ± SD, $n=50$)	Gold particels in the background[c] (mean ± SD, $n=25$)
N-1	66.9 ± 10.4	74.1 ± 8.7	3.8 ± 3.0
N-2	66.6 ± 11.4	73.7 ± 8.9	3.6 ± 2.7
HS-1	10.7 ± 5.9	62.5 ± 8.7	5.4 ± 3.1
HS-2	8.1 ± 6.2	53.6 ± 9.2	4.5 ± 2.9
HS-3	9.1 ± 6.5	52.8 ± 9.1	3.3 ± 2.0
HE-1	17.3 ± 6.0	48.1 ± 10.7	4.0 ± 2.9
HE-2	19.0 ± 6.9	64.1 ± 12.7	3.8 ± 2.7

Twenty-five erythrocytes for each case were measured to obtain the data.

[a] The number of intersections per 0.25 μm^2 cytoplasmic side was counted in three different areas of an erythrocyte

[b] The number of gold particles per 0.25 μm^2 cytoplasmic side was counted in two different areas

[c] The number of gold particles per 0.25 μm^2 outside was counted for 25 background areas

le 2b). The background number of gold particles is low among all cases (Table 2c).

Discussion

The ultrastructure of normal and abnormal erythrocyte membranes has been investigated by means of transmission and scanning electron microscopy (Burke and Shotton 1983; Fujikawa 1983; Hainsfeld and Steck 1977; Lupu and Constantinescu 1989; Tsukita et al. 1980). However, these studies have been fraught with technical problems. The specimens, prepared by conventionally used techniques including osmium fixation and dehydration steps, did not show the networks underlying the lipid erythrocyte membrane as they were in situ; these structures have inevitably undergone modification in fixation. Recently artificially spread networks were clearly shown in negatively stained preparations, but have not been seen in situ (Byers and Branton 1985; Liu et al. 1987; McGough and Josephs 1990; Shen et al. 1984, 1986). The erythrocyte splitting technique employed in the present study in combination with the quick-freezing and deep-etching method, has rendered it possible to remove the soluble proteins from erythrocytes and to obtain ultrastructural preparations showing the cytoplasmic aspect of erythrocyte membranes. Thus we could examine abnormally shaped erythrocytes.

The present morphological study demonstrated remarkable differences between normal erythrocytes and abnormally shaped ones. Abnormally shaped erythrocytes were shown to have structural changes on the cytoplasmic side of the erythrocyte membrane which were not observed in normal erythrocytes. These changes were characterized by diminished filamentous structures and a relative predominance of granular structures. From the report that spectrin dimers were more abundant in HE (Coetzer and Zail 1982; Liu et al. 1982), the ultrastructural changes in erythrocyte membranes of HE patients could be accounted for by the relative predominance of spectrin dimers over tetramers and a consequent defective organization of filamentous networks. However, the present study did not allow us to make a definitive statement on a similarity of the ultrastructure of the membrane in HS and HE. We speculate that the difference in the shape of erythrocytes between the two conditions depends on the degree to which components of the membrane skeleton are transformed from filamentous to granular.

In normal erythrocytes spectrin molecules are in their curved and/or shortened state and are thought to play an important role in imparting flexibility and deformability to the erythrocyte membrane (McGough and Josephs 1990). However, on the cytoplasmic aspects of erythrocyte membranes in HS, filamentous structures were found to be diminished and granular structures dominated. These changes seem to be attributable to an abnormality of membrane skeletal proteins (Delaunay et al. 1990; Goodman and Shiffer 1983; Iolascon et al. 1992), such as a defective binding of spectrin to band 4.1 (Goodman et al. 1982), quantitative decreases of spectrin (Agre et al. 1985, 1986) and a defective gene for ankyrin (Lux et al. 1990). Therefore, inadequacy of binding of membrane skeletal proteins and consequent inability of three-dimensional networks to be formed would result in weakening of the membrane-supporting power of the cytoskeleton.

Erythrocytes of HS and HE patients that had apparently assumed the normal discoid shape were also examined (unpublished data). Some showed a diminution of filamentous structures, with more granular structures, while others were of the same filamentous texture as normal erythrocytes. These findings did not permit us to draw any definitive explanation as to the abnormality of cytoplasmic aspects of all HE or HS erythrocytes.

The mechanism whereby defective binding of component proteins in the erythrocyte membrane causes the discoid erythrocyte to have a spherical or elliptic deformation is not understood. Morphological abnormalities probably result from many genetic defects, with each kindred carrying a different mutation (Delaunay et al. 1990; Goodman and Shiffer 1983). One of the mechanisms underlying morphological abnormalities here may be a defect of membrane skeletal proteins, a conclusion compatible with earlier results (Lui et al. 1990). It is suggested that a defect of the spectrin network may be the primary abnormality of HE or HS erythrocytes, a hypothesis which must be verified by further studies, including those on age-related structural changes in the cytoplasmic aspects of erythrocytes and by studies which are designed to explore membrane skeletons using immunostaining techniques for proteins such as actin, ankyrin, band 3 and band 4.1. From the present study it appears that one of the basic events in HS and HE is an alteration in the cytoplasmic aspects of erythrocyte membranes. These changes probably play a primary role in the causation of abnormality of shape of elliptocytic or spherocytic erythrocytes.

Acknowledgements. This work has been supported in part by a Grant-in-Aid for General Scientific Research, no. 3670007, given by The Ministry of Education, Science and Culture to S. Ohno.

References

Agre P, Casella JF, Zinkham WH, McMillan C, Bennett V (1985) Partial deficiency of erythrocyte spectrin in hereditary spherocytosis. Nature 314:380–383

Agre P, Asimos A, Casella JF, McMillan C (1986) Inheritance pattern and clinical response to splenectomy as a reflection of erythrocyte spectrin deficiency in hereditary spherocytosis. N Engl J Med 315:1579–1583

Bennett V (1985) The membrane skeleton of human erythrocytes and its implications for more complex cells. Annu Rev Biochem 54:273–304

Bennett V (1989) The spectrin-actin junction of erythrocyte membrane skeletons. Biochem Biophys Acta 988:107–121

Burke BE, Shotton DM (1983) Erythrocyte membrane skeleton abnormalities in hereditary spherocytosis. Br J Haematol 54:173–187

Byers TJ, Branton D (1985) Visualization of the protein associations in the erythrocyte membrane skeleton. Proc Natl Acad Sci USA 82:6153–6157

Coetzer T, Zail S (1982) Spectrin tetramer-dimer equilibrium in hereditary elliptocytosis. Blood 59:900–905

Delaunay J, Alloisio N, Morlé L, Pothier B (1990) The red cell skeleton and its genetic disorders. Mol Aspects Med 11:161–241

Fowler VM (1986) New views of the red cell network. Nature 322:777–778

Fujikawa S (1983) Tannic acid improves the visualization of the human erythrocyte membrane skeleton by freeze-etching. J Ultrastruct Res 64:289–298

Goodman SR, Shiffer K (1983) The spectrin membrane skeleton of normal and abnormal human erythrocytes: a review. Am J Physiol 244:C121–141

Goodman SR, Shiffer KA, Casoria LA, Eyster E (1982) Identification of the molecular defect in the erythrocyte membrane skeleton of some kindreds with hereditary spherocytosis. Blood 60:772–784

Hainsfeld JF, Steck TL (1977) The sub-membrane reticulum of the human erythrocyte: a scanning electron microscope study. J Supramol Struct 6:301–317

Iolascon A, Miraglia del Giudice E, Camaschella C (1992) Molecular pathology of inherited erythrocyte membrane disorders: hereditary spherocytosis and elliptocytosis. Haematologica (Pavia) 77:60–72

Liu SC, Palek J, Prchal JT (1982) Defective spectrin dimer-dimer association in hereditary elliptocytosis. Proc Natl Acad Sci USA 79:2072–2076

Liu SC, Derick LH, Palek J (1987) Visualization of the hexagonal lattice in the erythrocyte membrane skeleton. J Cell Biol 104:527–536

Liu SC, Derick LH, Agre P, Palek J (1990) Alteration of the erythrocyte membrane skeletal ultrastructure in hereditary spherocytosis, hereditary elliptocytosis, and pyropoikilocytosis. Blood 76:198–205

Lupu F, Constantinescu E (1989) A new freeze-drying device for platinum replica studies of cell surface and cytoskeleton: an example using immunogold-labeled human erythrocytes. J Electron Microsc Tech 11:76–82

Lux SE, Tse WT, Menninger JC, John KM, Harris P, Shalev O, Chilcote RR, Marchesi SL, Watkins PC, Bennett V, McIntosh S, Collins FS, Francke U, Ward DC, Forget BG (1990) Hereditary spherocytosis associated with deletion of human erythrocyte ankyrin gene on chromosome 8. Nature 345:736–739

Marchesi VT (1983) The red cell membrane skeleton: recent progress. Blood 61:1–11

McGough Am, Josephs R (1990) On the structure of erythrocyte spectrin in partially expanded membrane skeletons. Proc Natl Acad Sci USA 87:5208–5212

McGuire M, Agre P (1988) Clinical disorders of the erythrocyte membrane skeleton. Haematol Pathol 2:1–14

McGuire M, Smith BL, Agre P (1988) Distinct variants of erythrocyte protein 4.1 inherited in linkage with elliptocytosis and Rh type in three white families. Blood 72:287–293

Nermut MV (1981) Visualization of the "membrane skeleton" in human erythrocytes by freeze-etching. Eur J Cell Biol 25:265–271

Ohno S (1985) Immunocytochemical study on the cytoplasmic side of cell membrane infected with vesicular stomatitis virus by quick-freezing and deep-etching replica method. Histochemistry 82:565–575

Ohno S (1992) An ultrastructural study of the cytoplasmic aspects of erythrocyte membranes by a quick-freezing and deep-etching method. J Anat 180:315–320

Ohno S, Fujii Y (1990) Three-dimensional and histochemical studies of peroxisomes in cultured hepatocytes by quick-freezing and deep-etching method. Histochem J 22:143–154

Ohno S, Fujii Y (1991) Three-dimensional studies of the cytoskeleton of cultured hepatocytes: a quick-freezing and deep-etching study. Virchows Arch [A] 418:61–70

Ohno S, Takasu N (1989) Three-dimensional studies of cytoskeletal organizations in cultured thyroid cells by quick-freezing and deep-etching method. J Electron Microsc 38:352–362

Shen BW, Josephs R, Steck TL (1984) Ultrastructure of unit fragments of the skeleton of the human erythrocyte membrane. J Cell Biol 99:810–821

Shen BW, Josephs R, Steck TL (1986) Ultrastructure of the intact skeleton of the human erythrocyte membrane. J Cell Biol 102:997–1006

Tchernia G, Mohandas N, Shohet SB (1981) Deficiency of skeletal membrane protein band 4.1 in homozygous hereditary elliptocytosis. J Clin Invest 68:454–460

Tsukita S, Tsukita S, Ishikawa H (1980) Cytoskeletal network underlying the human erythrocyte membrane. J Cell Biol 85:567–576

Ursitti JA, Pumplin DW, Wade JB, Bloch RJ (1991) Ultrastructure of the human erythrocyte cytoskeleton and its attachment to the membrane. Cell Motil Cytoskeleton 19:227–243